CFD SIMULATION OF FLOW AND SEDIMENTATION IN CENTRIFUGAL FIELD

Dipl.-Ing. X. Romaní Fernández; Prof. Dr.-Ing. H. Nirschl
Institute of Mechanical Process Engineering and Mechanics,
Karlsruhe University, D-76131 Karlsruhe

ABSTRACT

The knowledge of the streams and the sedimentation behaviour inside a solid bowl centrifuge is decisive to find out the geometrical parameters that lead to an optimal performance. Due to the difficulty inherent in observing these phenomena inside the machines, the Computational Fluid Dynamics (CFD) becomes a relevant tool to research them. Considering the real centrifuge geometry, a three dimensional geometry was built and meshed. The CFD Software Fluent was then used to simulate the multiphase flow in the grid. For the calculation of the gas and liquid phase flow a Volume of Fluid approach was used. The Discrete Phase Model was applied to calculate the separation efficiency of the centrifuge by evaluating the trajectory of the solid particles.

KEYWORDS

Solid bowl centrifuge, CFD-Simulation, Multiphase Flow, Separation Efficiency.

1. Introduction

Solid-liquid separation is an important operation, especially in the industrial post-processing. Centrifuges can be used to separate fine solid particles from industrial fluids to increment its service life. Some examples are the cleaning of coolant lubricants in metal cutting, and in glass or ceramics processing, and the maintenance of chemical surface treatment baths. Among other centrifugal devices as decanters and disk stack separators, that are more complex, solid bowl centrifuges can be used to reach the mandatory clarifying purity.

Flow and sedimentation are well described in tubular centrifuges [1,2] and in overflow centrifuges [3], but the complex flow fields of industrial solid bowl centrifuges have not been amenable to rigorous mathematical analysis. The information about the flow inside these centrifuges and the influence of flow rate and bowl speed are decisive for an optimization in terms of geometry and process conditions. As the variety of simulation models and computing resources is raising, CFD tools for the development and optimization of industrial devices become more and more comfortable. Models of flow in some industrial process equipment have been developed using CFD and even some researchers have recently attempted to simulate the flow in centrifuges [4, 5, 6].

The aim of this study is the investigation of the multiphase flow in an industrial solid bowl centrifuge, which has radial compartments. The strategy followed is to solve numerically the governing flow equations with the software FLUENT. Particularly attention will be paid to the effect of the radial walls on the flow and therefore on the particle trajectories.

2. Model description

2.1 Mathematical formulation of the fluid

Computational Fluid Dynamics (CFD) solves the governing fluid flow equations, continuity and momentum conservation equations, by means of numerical methods. These partial differential equations are solved using the finite volume method integrated in the software FLUENT 6.3.26.

The Volume of Fluid (VOF) method, designed to track the interface of two phases that are not interpenetrating, simulates the gas-liquid multiphase flow. The presence of solid particles was ignored for flow simulation purposes, which is an acceptable assumption for low solid concentration. The VOF model tracks the interface between the gas and the liquid at each time t in a non-steady way. A continuity conservation equation (Eq.1) is solved for each phase, and the volume fraction of each phase α_q in any cell has to obey Eq.2,

$$\frac{\partial}{\partial t}\left(\alpha_q \rho_q\right) + \nabla \cdot \left(\alpha_q \rho_q \vec{v}_q\right) = 0, \tag{1}$$

$$\sum_{q=1}^{n} \alpha_q = 1. \tag{2}$$

As the flow inside the bowl is non-laminar, the Reynolds Averaged Navier-Stokes equation (Eq.3) was chosen to solve the velocity field. With the VOF method a single momentum equation is solved throughout the domain, and the resulting velocity field is shared among the phases. The dependency on the volume fraction is implemented by using volume averaged values for the density ρ and the viscosity μ,

$$\frac{\partial}{\partial t}\left(\rho \vec{v}\right) + \rho\left(\vec{v} \cdot \nabla\right)\vec{v} = -\nabla p + \nabla \cdot \tau + \nabla \cdot \tau_t + \vec{F}. \tag{3}$$

In Eq.1 and 3, v represents the velocity, p the pressure, τ the shear stress tensor, τ_t the tensor of turbulences and F an external volumetric force. All terms are discretized and calculated for each volume cell with the exception of τ_t, the tensor of turbulences, which is modelled via a k-ε model.

The k-ε model [7] requires two additional transport equations to model the turbulences, one for the turbulent kinetic energy, k, and another one for its rate of dissipation, ε. The advantage of this approach is the relatively low computational effort, the limitation of the model is the assumption that the turbulences are isotropic, which is not strictly true. The k-ε renormalization group (RNG), an extension of the standard k-ε model, takes into account the effect of swirl on turbulence, enhancing a higher accuracy for swirling flows. This model is more reliable for a wider class of flows than the standard k-ε model.

The equations 1-3 are solved based on a moving reference frame [7]; which is used to facilitate calculations in rotational systems.

2.2 Mathematical formulation of the particles

Once the flow has reached a quasi-steady state, which means that the interface between gas and liquid is stable and the outflow coincides the inflow, particle trajectories can be calculated. The Discrete Phase Model (DPM) available in Fluent is the tool of choice to face the calculation. In this model spherical particles are considered as discrete phase dispersed in the continuous phase in a Lagrangian

frame of reference. Adequate for low loaded flows, the Discrete Phase Model computes the current positions of particles integrating the force balance represented with Eq.4. This equation takes into account the discrete phase inertia, the hydrodynamic drag, the force of gravity and the rotational forces.

$$\frac{d\vec{v}_p}{dt} = F_D\left(\vec{v} - \vec{v}_p\right) + \frac{\vec{g}\left(\rho_p - \rho\right)}{\rho_p} + \vec{F}_r . \tag{4}$$

In Eq.4 v, v_p, ρ and ρ_p stand for the fluid velocity, particle velocity, the fluid density and particle density respectively.

The first term on the right side of Eq.4 constitutes the drag force per unit particle mass and the coefficient F_D is calculated with Eq.5. In order to calculate the drag coefficient C_D the approach for spherical particles described by Morsi and Alexander [8] was chosen. The relative Reynolds number, Re, is defined in Eq.6.

$$F_D = \frac{18\mu}{\rho_p d_p^2}\frac{C_D\,Re}{24} \tag{5}$$

$$Re = \frac{\rho\, d_p \left|v_p - v\right|}{\mu} \tag{6}$$

As the centrifuge rotates with an angular velocity Ω about the z-axis, the forces on the particles in x and y direction are given by Eq.7-8. The rotational forces include the centrifugal force (first term) and the Coriolis force (second term), which arises in the moving reference frame.

$$F_x = \left(1 - \frac{\rho}{\rho_p}\right)\Omega^2 x + 2\Omega\left(v_{y,p} - \frac{\rho}{\rho_p}v_y\right) \tag{7}$$

$$F_y = \left(1 - \frac{\rho}{\rho_p}\right)\Omega^2 y + 2\Omega\left(v_{x,p} - \frac{\rho}{\rho_p}v_x\right) \tag{8}$$

The dispersion of particles due to the turbulent eddies in the continuous phase can be predicted using a stochastic tracking model. The Random Walk Model (RWM), a stochastic tracking model in FLUENT, includes the effect of instantaneous turbulent velocity fluctuations on the particle trajectories through the use of stochastic methods. The particles interact with a succession of turbulent eddies characterized by a random velocity fluctuation u´, v´ and w´ and a time scale τ_e. The velocity fluctuations are proportional to a normally distributed random number ζ (Eq.9).

$$u' = \zeta\sqrt{\overline{u'^2}} \tag{9}$$

Since the turbulent kinetic energy, k, is known at each cell in the fluid, the velocity fluctuation can be defined for the k-ε model as in Eq.10:

$$\sqrt{\overline{u'^2}} = \sqrt{\overline{v'^2}} = \sqrt{\overline{w'^2}} = \sqrt{2k/3} . \tag{10}$$

The characteristic lifetime of the eddy τ_e is defined as a constant given by Eq.11 for the k-ε model.

$$\tau_e = 0{,}30\,k/\varepsilon \tag{11}$$

One limitation of the DPM is the restriction to particle phase with low concentration. The trajectory of the particles will be tracked until they reach the bowl wall (settled particles) or leave the domain with the outlet flow (not settled particles). In order to consider the sediment formation, an extra force has to be implemented by the user. This force should take into account particle-particle interactions during settling and in the sediment. Some efforts have been done to extend Eq.4 with a Soft Sphere Model [9].

Another limitation is that the DPM does not consider the interface tracked by the VOF model and, therefore, the wetting force that hinders the particles to travel from the liquid to the gas phase.

The tracking of submicron particles represents another problem. For these particles other forces not considered in Eq.4, as electrostatic forces and particle-particle interaction forces, play an important role.

2.3 Geometry and Mesh

Based on the real geometry of an industrial solid bowl centrifuge (Fig.1) a three dimensional geometry (Fig.2), representing one fourth of the bowl, was build and meshed. Because of the periodically repeating nature of the system only one fourth of the centrifuge was calculated. This geometry takes into account the inlet accelerator, the radial walls and the dimensions of the real bowl.

After some efforts with different grid resolutions, a mesh with approximately 800000 tetrahedral cells was used. The grid was refined at the bowl wall and at the radial walls to capture high velocity gradients.

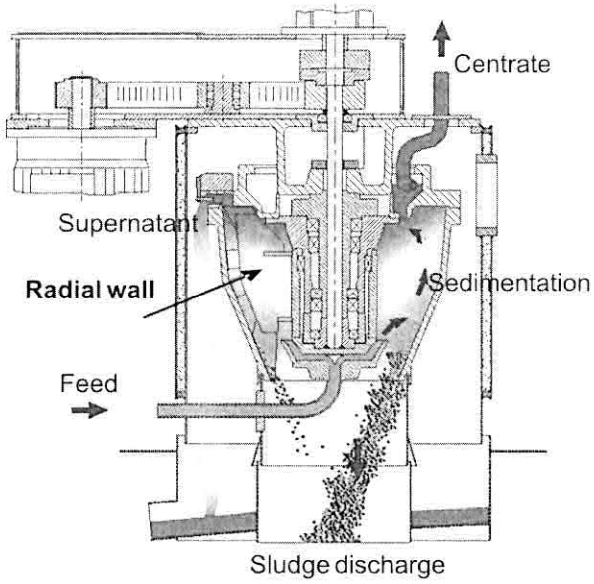

Fig.1. Centrifuge A-25 from the company STA (Separatoren-Technik und Anlagenbau)

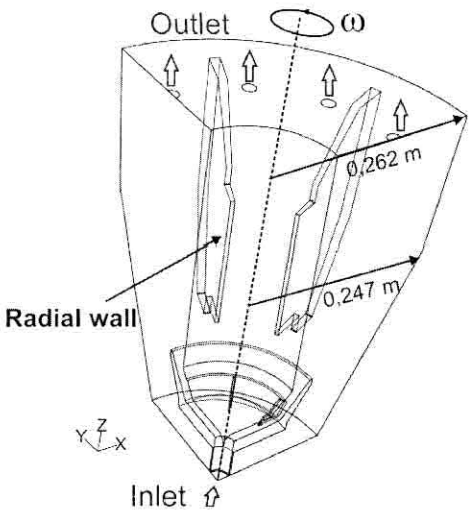

Fig.2. Geometry used for the simulation.

The liquid enters the centrifuge through the inlet flowing then into an accelerator, which consists of two rotating plates. Side and top walls of the bowl, defined with no-slip condition, rotate with the same angular velocity as the plates. The fluid leaves over a weir at the outlet; there atmospheric pressure was imposed as boundary condition. For the periodic surfaces, a periodic boundary condition was defined. This boundary condition uses the flow conditions at one of the periodic surfaces as its cells were the adjacent cells of the other periodic plane.

To simplify the simulation, the air is considered as an incompressible gas. This is a reasonable assumption for the operation conditions of atmospheric pressure and for a non-temperature dependent problem. The water is defined as an incompressible Newtonian fluid.

2.4 Validation

Since the measurement of the velocity components inside the solid bowl is not possible yet, the validation of the results is performed via comparison of the simulated and the experimental grade efficiency. The grade efficiency characterizes the quality of the solid-liquid separation as a function of the particle size. The grade efficiency for a certain particle size x is defined as the ratio between the amount of particles of size x which have settled and the amount of particles of this size which were present in the inlet flow (Eq.12).

$$\text{Grade efficiency}(x) = \frac{N_{p\_wall}(x)}{N_{p\_inlet}(x)} \tag{12}$$

3. Results

3.1. Gas-Liquid interface

The obtained gas-liquid interface is relatively sharp and it shows a profile with nearly constant radius along the length. The position of the gas-liquid interface is determined by the weir position, the rotation speed and the inlet flow rate. As shown in Fig.3, there is a rotating water pool at the bowl wall around an air core. Water is fed axially through the inlet to the accelerator; there the water changes its direction and gains in tangential velocity. Then, a jet of water exits the accelerator and enters the rotating liquid pool. Because of the Coriolis force, the liquid jet describes a spiral path contrary to the rotation of the centrifuge. Pictures made during the experiments reveal that this phenomenon occurs.

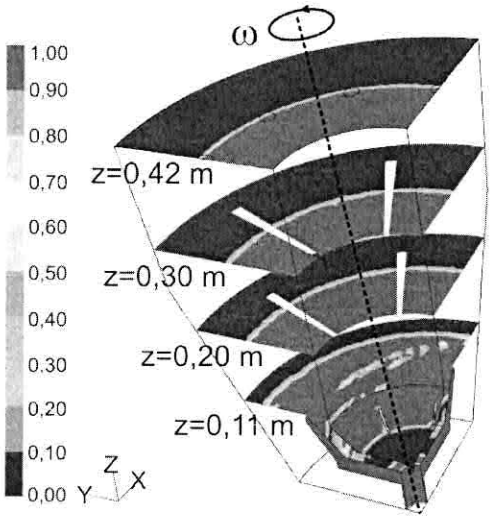

Fig.3. Contours of volume fraction (air).

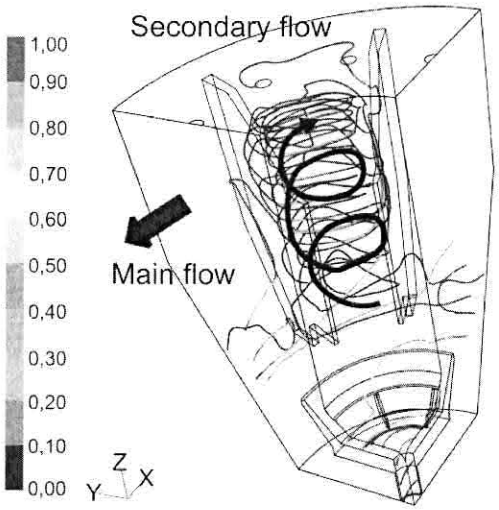

Fig.4. Relative path line coloured by volume fraction (air).

3.2. Flow patterns

The main flow occurs in the direction of the rotation speed of the bowl; both the liquid pool and the air core rotate. Nevertheless, the radial walls cause a secondary flow

between them. Fig.4 shows the relative path line made by a massless particle of water coming from the inlet and leaving the centrifuge through the weir. The water describes a spiral path between the walls whereas it rotates around the axis.

The tangential velocity of the rotating water achieves the velocity corresponding to a rigid body motion (
Fig.5). The liquid jet coming from the inlet accelerator has a lower tangential velocity than the rotating liquid pool when entering it. This underaccelerated inlet flow would cause a slow down on the rotating pool if the radial walls were not there. Therefore the tangential velocity in previous simulations of the same solid bowl without the radial walls [10] is lower than the rigid body motion.

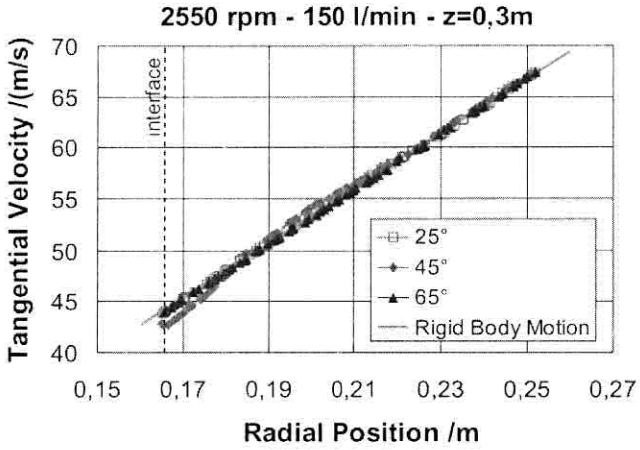

Fig.5. Tangential velocity of water versus radius for different angular positions: behind (25°), between (45°) and in front of the radial walls (65°) at the height of z=0,3m.

Operation conditions: flow rate 150 L/min and angular speed 1000 rpm.

The other effect produced by the radial walls is the spiral flow between them. Considering a horizontal surface, for example with a height of z=0,2m (
Fig.6), a radial flow can be observed between the walls in the same direction as the rotation speed of the centrifuge. In front of the radial walls (angular positions 20° and 65°) the radial velocity is positive, and it turns negative behind the radial walls (angular position 25° and 70°). A positive radial velocity means that the flow is directed to the bowl wall and a negative one means that the flow occurs in the opposite direction. In the middle of the walls (angular position 0° and 45°) there is no radial movement and the radial velocity is approximately zero.

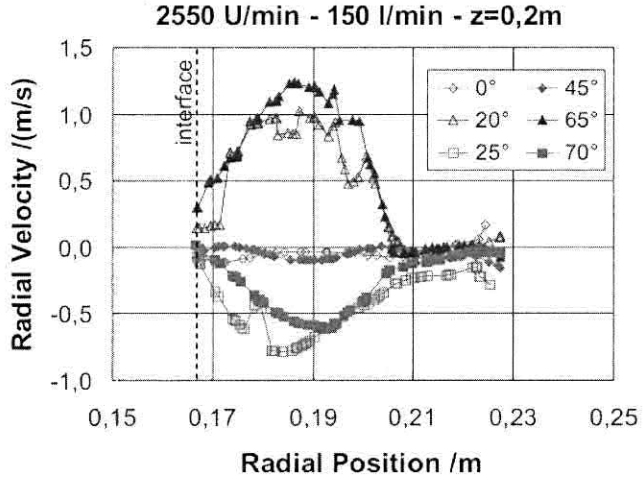

Fig.6. Radial velocity of water versus radius for different angular positions: behind (25°, 70°), between (0°, 45°) and in front of the radial walls (20°, 65°) at the height of z=0,2m.

Operation conditions: flow rate 150 L/min and angular speed 1000 rpm.

Regarding the axial flow, the spiral path disturbs the boundary layer of fast moving fluid at the gas-liquid interface observed in the simulations without the radial walls

[10], and researched in literature of tubular and overflow centrifuges [2][11]. Instead, an irregular layer at the interface is formed and other regions of the flow, such as in front of the walls, acquire positive axial velocity.

3.3. Particle traces

Once the flow simulation has converged, particles with different diameters (from 10 µm to 0,5 µm) and 2650 kg/m^3 density were introduced in the domain at the point where the liquid enters the rotating pool. Their trajectories were traced using Eq.4. The simulation results show particles rotating around the axis, as the tangential movement superposes axial and radial movements. Due to the centrifugal force, big particles move radially towards the wall to settle there (Fig.7, 10 µm particle). Small particles get captured by the spiral flow, which hinders its sedimentation. Some of them reach the wall (Fig.7, 5 µm particle), but the other escape through the weir following the flow (Fig.7, 1 µm particle). The radial walls should lead to an improvement in the grade efficiency compared to the centrifuge without them [10] because the radial walls improve the acceleration of the fluid and, therefore, the acceleration of the particles. But they are also responsible for secondary streams that reduce the settle rate for small particles. An optimum regarding the geometry and the number of radial walls has to be found.

After tracking the particles, the grade efficiency for each particle diameter was calculated with Eq.12. This value can be compared with the grade efficiency reached during the experiments performed by the same operation conditions (Fig.8). Simulated and experimental values of grade efficiency agree with each other for big particles. Differences appear for particles smaller than 2 µm. On the one hand, the small particles go to the air phase because the force at the interface caused by the surface tension is not considered in Eq.12. On the other hand, electrostatic forces and particle-particle interaction forces, which are not taken into account in the current calculation, play a major role for submicron particles.

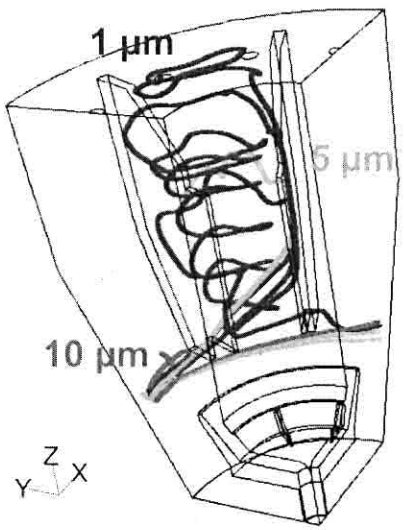

Fig.7. Particle traces coloured by particle diameter (m) at 1000 rpm and 150 L/min inlet flow.

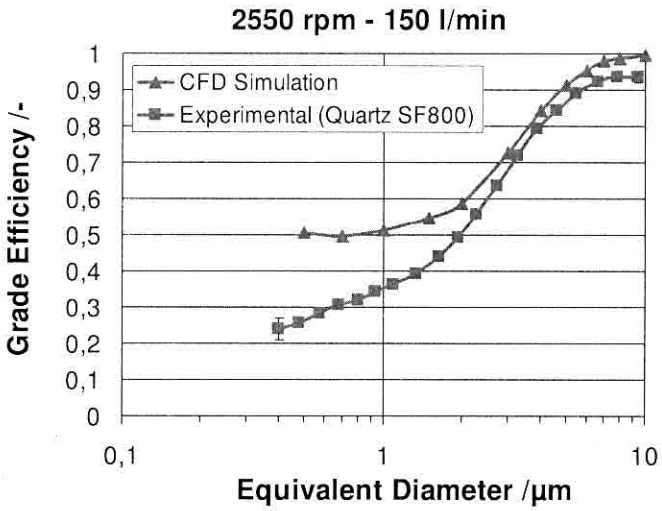

Fig.8. Grade Efficiency calculated with Eq.12 from the simulated particle traces and from the experiments.

4. Conclusions

CFD simulations of the multiphase flow in a solid bowl centrifuge with radial walls were successfully performed with the software FLUENT. A relative sharp gas-liquid interface was obtained using the Volume of Fluid (VOF) model. The main flow of water takes place in tangential direction and reaches the rigid body motion thanks to the extra acceleration of the radial walls. A secondary flow, spirally between the radial walls, occurs towards the outlet weir. The radial walls are helpfully for the acceleration and should improve the separation efficiency; but they originate a secondary flow which hinders the sedimentation of small particles.

Particles with diameters from 10 µm to 0,5 µm were tracked using the Discrete Phase Model. Simulated and experimental grade efficiency agrees with each other for particles bigger than 2 µm. For smaller particles the implementation of a wetting force at the interface is required.

5. References

[1] E. Bass, *Strömungen im Fliehkraftfeld I*, Periodica polytechn. 3 (1959) 321-339.

[2] W. Gösele, *Schichtströmung in Röhrenzentrifugen*, Chemie-Ing.-Techn. 40. Jahrg., Heft 13 (1968) 657-659.

[3] H. Reuter, *Strömungen und Sedimentation in der Überlaufzentrifuge*, Chemie-Ing.-Techn. 39. Jahrg., Heft 5/6 (1967) 311-318.

[4] M. Boychyn, S.S.S. Yim, P. Ayazi Shamlou, M. Bulmer, J. More, M. Hoare, *Characterization of flow intensity in continuous centrifuges for the development of laboratory mimics*, Chemical Engineering Science 56 (2001) 4759-4770.

[5] M. Jain, M. Paranandi, D. Roush, K. Göklen, W.J. Kelly, *Using CFD to Understand How Flow Patterns Affect Retention of Cell-Sized Particles in a Tubular Bowl Centrifuge*, Ind. Eng. Chem. Res., 44 (2005) 7876-7884.

[6] K.E. Wardle, T.R. Allen, *Computational Fluid Dynamics (CFD) Study of the flow in an Annular Centrifugal Contactor*, Separation Science and Technology, 41 (2006) 2225-2244.

[7] Fluent 6.3 Documentation, User's guide (2006).

[8] S. Morsi, A. Alexander, *An Investigation of Particle Trajectories in Two-Phase flow Systems*, Fluid Mech. 55 (1972) 193-208.

[9] K.W. Chu, A.B. Yu, *Numerical simulation of complex particle-fluid flows*, Powder Technology, 179 (2008) 104-114.

[10] X. Romani, H. Nirschl, *Multiphase CFD Simulation of a Solid Bowl Centrifuge*, Chemical Engineering & Technology, 32, 5, (2009) 719-725.

[11] U. Glinka, Die Strömung in Überlaufzentrifugen – Neue Ergebnisse mit einem elektrolytischen Markierungsverfahren, Verfahrenstechnik, 5, (1983) 315-319.